Accepted Manuscript

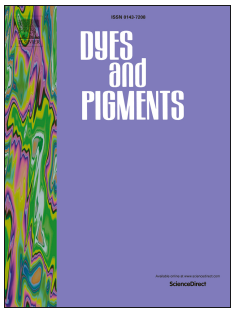

Investigation of novel substituted zinc and aluminium phthalocyanines for photodynamic therapy of epithelial breast cancer

Imadadulla Mohammed, David O. Oluwole, Manjunatha Nemakal, Lokesh Koodlur Sannegowda, Tebello Nyokong

PII: S0143-7208(19)30545-5

DOI: https://doi.org/10.1016/j.dyepig.2019.107592

Article Number: 107592

Reference: DYPI 107592

To appear in: *Dyes and Pigments*

Received Date: 11 March 2019

Revised Date: 30 April 2019

Accepted Date: 28 May 2019

Please cite this article as: Mohammed I, Oluwole DO, Nemakal M, Sannegowda LK, Nyokong T, Investigation of novel substituted zinc and aluminium phthalocyanines for photodynamic therapy of epithelial breast cancer, *Dyes and Pigments* (2019), doi: https://doi.org/10.1016/j.dyepig.2019.107592.

Synthesis of novel substituted zinc and aluminium phthalocyanines for photodynamic therapy of epithelial breast cancer

Imadadulla Mohammed[a], David O. Oluwole[b], Manjunatha Nemakal[a], Lokesh Koodlur Sannegowda*[a], Tebello Nyokong*[b].

[a]Department of Chemistry, Vijayanagara Sri Krishnadevaraya University, Vinayakanagara, Ballari-583105, Karnataka, INDIA

[b]Center for Nanotechnology Innovation, Department of Chemistry, Rhodes University, Grahamstown 6140, South Africa

Table of Content Graphic

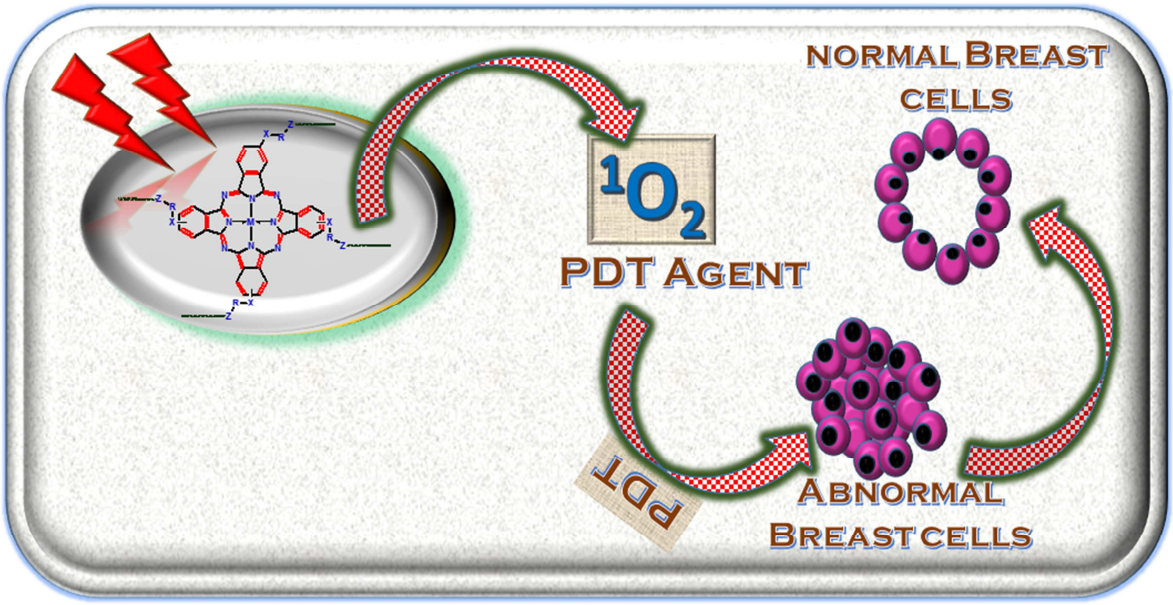

Investigation of novel substituted zinc and aluminium phthalocyanines for photodynamic therapy of epithelial breast cancer

Imadadulla Mohammed[a], David O. Oluwole[b], Manjunatha Nemakal[a], Lokesh Koodlur Sannegowda*[a], Tebello Nyokong*[b].

[a]Department of Chemistry, Vijayanagara Sri Krishnadevaraya University, Vinayakanagara, Ballari-583105, Karnataka, INDIA

[b]Center for Nanotechnology Innovation, Department of Chemistry, Rhodes University, Grahamstown 6140, South Africa

Abstract

A series of phthalonitrile ligands were synthesized by nucleophilic substitution reaction using the hydroxyl or sulfanyl group precursors and the nitro moiety of the nitrophthalonitrile to yield corresponding oxy or sulfanyl bridged ligands. These ligands were subsequently subjected to cyclocondensation reaction with diamagnetic metal ions like zinc and aluminium to afford symmetrical substituted zinc and aluminium phthalocyanine (Pc) complexes and polymers. The ligands and Pc complexes were characterized by ^{1}H-nuclear magnetic resonance, fourier transform infrared, ultraviolet visible and mass spectrometric techniques. Additionally, thermal gravimetric, and elemental analyzer were used for characterization of the Pc complexes. The photophysical and photochemical behaviour of the Pc complexes were investigated in dimethyl sulfoxide. Additionally, the complexes were tested against epithelial breast cancer cells for photodynamic therapy (PDT) effect. The substituted ZnPc complexes afforded higher singlet oxygen quantum yields as compared to the AlPc analogue. All the complexes showed innocuous *invitro* dark cytotoxicity and moderate PDT effect.

Key words: Zn phthalocyanine, Al phthalocyanine, polymer, amide bond, singlet oxygen quantum yield, photodynamic therapy.

*Corresponding authors: kslokesh@vskub.ac.in; T.nyokong@ru.ac.za

1. Introduction

Metallophthalocyanines (MPcs) are conjugated planar aromatic macrocycles having 18π–electron ring system with four isoindole units linked via nitrogen atoms [1, 2]. MPcs offer structural flexibility according to the utility and application by tailoring the Pc ring with different functionality leading to improved solubility. Different MPcs can be synthesized by altering the central metal cations at the core structure [3-6]. Phthalocyanine moiety has sufficient space to accommodate metal cations in its central cavity.

Nowadays, MPcs and their derivatives have been frequently used in photodynamic therapy (PDT) [7-10]. The singlet oxygen species are considered as the major cytotoxic species responsible for photodynamic therapy (PDT) effect against tumorigenic cells. Typically, the photosensitizer (PS) gets excited to its triplet state by light of appropriate wavelength (630-800 nm) and the excited PS interacts with its environment to produce highly reactive intermediates (singlet oxygen, superoxide anion, and hydroxyl radical) that are cytotoxic leading to tumor regression either directly by cell inactivation and/or indirectly by the destruction of the tumor vascular microcirculation [9-11]. Most of the PS used in PDT [12-14] are tetrapyrrolic in nature; chlorin, porphyrin, phthalocyanine and bacteriochlorin. Among these, MPcs are known for their minimal dark cytotoxicity and efficacious PDT activity [15]. Especially Pc derivatives with diamagnetic metal ions like zinc and aluminium have been explored for PDT because of their ability to generate high singlet oxygen quantum yield which are essential for PS application in PDT [16,-18]. Hence, there are lot of reports and efforts to enhance the efficiency of the singlet oxygen production by tuning and modifying the functional groups at the periphery of the Pc macrocycle [19]. Herein, we report for the first time the synthesis of MPc complexes with different peripheral functionalities, namely zinc tetra 3-[(4-nitrophenyl)amino]-1-phenylpropan-1-one-3-(phenoxy) phthalocyanine **[Pc 1],** tetra 3-amino-propan-1-one-1,3-bis(phenoxy) zinc phthalocyanine polymer **[Pc 2]**, zinc tetra 4-(4-(p-tolyimino)methyl)phenoxy phthalocyanine

[Pc-3], tetra (E)-(naphthalen-1-yl)({4-[(E)-2-(naphthalen-1-yl)diazen-1-yl]phenyl})diazene-bis(oxy) zinc phthalocyanine polymer **[Pc 4],** tetra 3H-spiro[2-benzofuran-3,9'-xanthene]-3-one-3',6'-bis(oxy) zinc phthalocyanine polymer **[Pc 5],** zinc tetra 2-methylpropanoic acid-2-oxy phthalocyanine **[Pc 6]** and aluminium-chloro tetra pyridin-1-ium-1-olate-2-sulfanyl phthalocyanine [**Pc 7]**. The efficiency of the MPcs with different functionalities were systematically investigated for their singlet oxygen production and PDT effect.

2. Materials and Methods:

4-Nitrophthalonitrile, ammonium molybdate, urea, $ZnCl_2$, $AlCl_3$, P-phenylenediamine, p-hydroxybenzaldehyde, 4-hydroxyacetophenone, citric acid, 2-naphthol, 2-mercaptopyridine-N-oxide, α-hydroxyisobutyric acid, 4-nitroaniline, P-toludine, N,N-dimethylformamide, n-pentanol, methanol, ethanol, spectroscopy grade dimethyl sulfoxide (DMSO), 1,3–diphenylisobenzofuran (DPBF) and unsubstituted zinc phthalocyanine were acquired from Sigma Aldrich®. Cultures of human breast adenocarcinoma cells (MCF–7) were obtained from Cellonex®. Dulbecco's modified Eagle's medium (DMEM) with phenol red, phenol red free DMEM, trypan blue, Dulbecco's phosphate–buffered saline (DPBS) and trypsin were purchased from Sigma Aldrich®. 100 µg/mL–Penicillin–100 unit/mL–streptomycin–amphotericin B mixture, heat-inactivated fetal bovine serum (FBS) were acquired from Biowest®. Cell proliferation neutral red reagent WST–1 (Roche®), 96 well cell culture plates (Nest®), 25 cm^2 and 75 cm^2 vented flasks were obtained from Porvair®.

2.1 Equipment:

Vario EL III CHNS elemental analyzer was used for the determination of elemental compositions (C, H, N, S) of the synthesized complexes. Absorption spectra were recorded on a Perkin Elmer Lambda 950 spectrophotometer for the Pc complexes. FTIR spectra were recorded as KBr pellet in 4000 to 500 cm^{-1} using Perkin Elmer Spectrum-Two spectrophotometer. Thermogravimetric analysis was carried out on a STA6000 machine in the temperature range 30 to 700 $^{\circ}C$ in oxygen atmosphere. The ^1H NMR spectra were recorded on a Bruker AMX-400 using either deuterated methanol (MeOD-d4) or DMSO-d6 or $CDCl_3$ solvent and mass spectra

were recorded on Bruker ESQUIRE 3000 Mass Spectrometer using MS (ESI) technique for the ligands and phthalocyanine molecules.

Illuminations for singlet oxygen quantum yields were performed using a general electric quartz lamp (300 W). A 600 nm glass cut off filter (Schott®) and water filter were employed to filter off ultra-violet and infrared radiation, respectively. An interference filter, 670 nm with a bandwidth of 40 nm, was placed in the light path between the sample holder and 600 nm glass cut off filter. Light intensities were measured with a POWER MAX 5100 (Molelectron® detector incorporated) power meter and were found to be 4.3×10^{15} photons cm^{-2} s^{-1}. For the singlet oxygen generation studies, samples and standards were mixed with the singlet oxygen quencher (~ 3 x 10^{-5} mol dm^{-3} DPBF was used for all mixtures, to avoid chain reactions) in DMSO at a mixing ratio of 1:1 and the depletion of the quencher in the presence of samples or standard was spectroscopically monitored at ~417 nm using a predetermined time intervals. The rate of the photodegradation of the quencher in the presence of samples or standard was used in the determination of the singlet oxygen quantum yields. Fluorescence excitation and emission spectra were measured on a Varian Eclipse® spectrofluorometer using a 360–1100 nm filter, absorbance at the excitation wavelength was adjusted to ~0.05. Fluorescence lifetimes were measured using a time correlated single photon counting setup (TCSPC) (FluoTime 300, Picoquant® GmbH) with a diode laser (LDH–P–670, Picoquant® GmbH, 20 MHz repetition rate, 44 ps pulse width) [20].

Illumination source for PDT studies was obtained from Modulight® Medical Laser system (ML) 7710–680 channel Turnkey laser system coupled with a 2 × 3 W channel at 680 nm, cylindrical output channels, aiming beam, integrated calibration module, foot/hand switch pedal, subminiature version A connectors and safety interlocks. Illumination kit for *in vitro* PDT studies has capacity to hold 127.76 × 85.48 mm 96 well cell culture plate [21].

The MCF–7 cells were cultured in 25 cm^2 and 75 cm^2 vented flasks (Porvair®) in a humidified atmosphere incubator with ~5% CO_2 and physiological temperature of 37 °C (HealForce®). The cells were viewed under phase contrast using a Zeiss® AxioVert. A1 Fluorescence LED (FL–LED) inverted microscope and the cell viability was measured using cell proliferation neutral red reagent WST–1 (Roche®) with a Synergy 2 multi–mode microplate reader (BioTek®).

2.2. Synthesis of substituted phthalonitrile ligands:

*2.2.1. Synthesis of 3-(4-hydroxy-phenyl)-3-(4-nitro-phenylamino)-1-phenyl-propan-1-one (**i**):*

The mixture of 4-nitroaniline (3 g, 21 mM), acetophenone (2.5 g, 21 mM), p-hydroxybenzaldehyde (2.6 g, 21 mM) and citric acid (0.8 g, 20 mM) were charged into a flask containing 10 mL ethanol [22, 23]. The reaction mixture was stirred at room temperature for 24 h. The reaction was monitored by TLC. After the reaction completion, the crude product was cooled to room temperature and poured into beaker containing ice water, the precipitate obtained was filtered and washed with excess of deionized water until it was free from acid. The crude product was purified by recrystallization from aq. ethanol. The resultant product was dried over P_2O_5. Yield. 85%. Melting point. 122 $^{\circ}$C.

FTIR (cm^{-1}): 1550 (C=C stretching), 1700 (-C=O stretching), 2890 (C-H stretching) and 3200-3550 (-OH stretching).

^{1}H-NMR(300 MHz, MeOD): δ 8.04-7.63 (m, 4 Ar-H), δ 7.58-7.30 (m, 4 Ar-H), δ 7.14 (d, J = 8.8 Hz, 1H), 6.75 (d, J = 8.8 Hz, 1H), δ 6.68-6.60 (m, 1H) δ 6.41 (m, 2H) 5.01 (dd, J= 5, 8.4 Hz, 1H), 3.54 (dd, J= 8.4, 17.0 Hz, 1H), δ 3.38-3.25 (m, 1H), δ 2.26-2.60 (m, 1H) .
Anal. For: $C_{21}H_{18}N_2O_4$: Calc. C, 69.60; H, 5.01; N, 7.73; O, 17.66. Found: C, 70.00; H, 4.80; N, 7.40.

MS (ESI): calc: 362.3 for $C_{21}H_{18}N_2O_4$; m/z: 380 $[M +H+NH_3]^+$, 317 $[M+H-NO_2]^+$.

*2.2.2. Synthesis of 4-{4-[1-(nitro-phenylamino)-3-oxo-3-phenyl-propyl]-phenoxy}-phthalonitrile (**ii**):*

Compound **i** (5.0 g, 0.0139 M) and 4-nitrophthalonitrile (2.4 g, 0.0139 M) were dissolved in 20 ml of DMF and K_2CO_3 (1.93 g, 0.039 M) was added to the mixture in three portions within 30 min. with continuous stirring at room temperature. The reaction mixture was maintained at room temperature and stirred for 72 h under inert atmosphere. Completion of the reaction was confirmed by TLC and the product was poured into ice water with constant stirring to yield brownish precipitate. The precipitate was washed with excess of deionized water and dried. The crude product was recrystallized from ethanol and dried over P_2O_5. Yield: 80%. Melting point. 104 $^{\circ}$C.

FTIR (cm^{-1}): 1560 (C=C stretching), 1692 (C=O stretching), 2915(C-H stretching), 2224 (-CN stretching), and 3365 (-NH stretching).

^{1}HNMR: (400 MHz, $CDCl_3$): δ 1.24 (s, 2H), 3.48 (d, J = 8.0 Hz, 1H), 5.03 (s, 1H), 6.48 (d, J=8.0 Hz, 1H), 6.62 (d, J= 7.5 Hz, 1H), 6.79 (d, J=8.0 Hz, H), 7.23 (d, J= 7.5 Hz, 2H), 7.41 (d, J= 1.2 Hz, 2H), 7.55 (d, J= 8.0 Hz, 2H), 7.74 (d, J=8.0 Hz, 2H), 8.00 (dd, J= 1.6, 8.4 Hz, 1H), 8.58 (d, J= 8.0Hz, 2H), 8.65 ppm (d, J= 8.0 Hz, 1H).

Anal. For $C_{29}H_{20}N_4O_4$: Calc. C, 71.30; H, 4.13; N, 11.47; O, 13.10. Found: C, 70.90; H, 4.54; N, 11.57.

*2.2.3. Synthesis of 3-amino-1,3-bis(4hydroxyphenyl]propane-1-one (**iii**):*

The mixture of 4-hydroxyacetophenone (3.0 g, 22 mM), vaniline (3.35 g, 22mM), ammonia (0.27 ml, 22 mM) and citric acid (0.8 g, 20mM) were transferred into a flask containing 10 ml of ethanol and the reaction mixture was stirred at room temperature for 24 h. Upon reaction completion, the mixture was poured into the beaker containing ice water and the obtained precipitate was filtered and washed with excess of deionised water until it is free from acid. The product was recrystallized from aq. ethanol. The resultant product was dried over P_2O_5. Yield. 85%. Melting point. 72 $^{\circ}$C.

FTIR (cm^{-1}): 1580 (C=C stretching), 1680 (C=O stretching), 2900 (C-H stretching) and 3210-3500 (-OH stretching).

^{1}H-NMR (400 MHz, DMSO-d6): δ 2.10 (d, J=7.3 Hz, 2H), 3.50 (s, 1H), 4.80 (d, J=7.3 Hz, 2H), 5.08 (br s, 2H), 6.40-7.00 (m, 4H), 7.02 (d, J=7.0 Hz, 2H), 8.15 (d, J=7.0 Hz, 2H).
Anal. For: $C_{15}H_{15}NO_3$: C, 70.02; H, 5.88; N, 5.44; O, 18.66. Found: C, 69.82; H, 5.68; N, 5.84.

*2.2.4. Synthesis of 4-(4-{1-amino-3-[4-(3,4-dicyanophenoxy)phenyl]-3-oxopropyl}phenoxy)benzene-1,2-dicarbonitrile (**iv**):*

Compound **iv** was synthesised using the procedure employed for compound **ii** but compound **iii** was used instead of **i**. The precipitate was washed with excess of deionized water and the crude product was recrystallized from ethanol and dried over P_2O_5. Yield: 80%. Melting point. 117 $^{\circ}$C

FTIR (cm^{-1}): 1553(C=C stretching), 1650 (C=O stretching), 2930 (C-H stretching), 2232 (-CN stretching), and 3330 (-NH_2 stretching).

^{1}H-NMR (400 MHz, DMSO-d6): δ 1.24 (d, J=7.3 Hz, 1H), 2.59 (d, J=7.3 Hz, 2H), 3.83 (s, 2H), δ 7.29-7.35 (m, 3H), 7.36-7.44 (m, 2H), 7.46-7.53 (m, 1H), 7.65-7.71 (m, 2H), 7.80 (d, J = 2.4

Hz, 1H), 7.94 (d, J = 2.4 Hz, 1H), 8.07 (d, J = 8.8 Hz, 1H), 8.10-8.14 (m, 4H), 8.17 (d, J = 8.0 Hz, 2H).

Anal. For $C_{32}H_{21}N_5O_4$: Calc. C, 71.24; H, 3.92; N, 12.98; O, 11.86. Found: C, 70.86; H, 4.15; N, 13.32.

MS (ESI)***:*** calc: 540.44 for $C_{32}H_{21}N_5O_4$; m/z: 541 $[M + H]^+$.

*2.2.5. Synthesis of 4-(p-tolyimino) methyl) phenol (**v**):*

A mixture of p-hydroxy benzaldehyde (2.0 g, 0.016 M) and p- toluidine (1.75 g, 0.016 M) were dissolved in 10 mL of methanol and 0.2 mL of triethylamine was added to the mixture. The reaction mixture was refluxed with constant stirring for 4 h to form light yellow colour product. The crude product was recrystallized to form a pure (E)-4-(p-tolyimino) methyl) phenol. Yield: 80%. Melting point. 149 $^{\circ}$C**.**

FTIR (cm^{-1}): 1545 (C=C stretching), 1600 (C=N stretching), 2890 (C-H stretching) and 3010-3250 (-OH).

^{1}H-NMR (400 MHz, DMSO-d6): δ 2.10 (s, 3H), 4.90 (br s, 1H), 7.05 (d, J= 7.2 Hz, 2H), 7.21-7.23 (m, 4H), 7.48 (d, J= 7.2 Hz, 2H), 8.64 (s, 1H).

Anal. for: $C_{14}H_{13}NO$: Calc. C, 79.59; H, 6.20; N, 6.63; O, 7.57. Found: C, 79.35; H, 6.32; N, 6.75.

*2.2.6. Synthesis of 4-(4-(p-tolyimino)methyl)phenoxy phthalonitrile (**vi**):*

Compound **vi** was synthesized using the same protocol applied for compound **ii** but compound **v** was used instead of **i.** After the completion of the reaction, the product was extracted with ethylacetate and washed with water. The organic layer was separated and dried over anhydrous Na_2SO_4. Yield: 70%. Melting point. 132 $^{\circ}$C.

FTIR (cm^{-1}): 1610 and 1475 (C=C stretching), 3030 (C-H stretching) and 2230 (-CN stretching).

^{1}H-NMR (400 MHz, DMSO-d6): δ 2.30 (s, 3H), 7.44 (dd, J= 1.6, 8.4 Hz, 1H), 7.91 (d, J= 8.0 Hz, 2H), 7.94 (d, J= 1.2 Hz, 1H), 8.16 (d, J= 7.0 Hz, 1H), 8.50 (s, 1H).

Anal. For $C_{22}H_{15}N_3O$: Calc. C, 78.3; H, 4.48; N, 12.46; O, 4.74. Found: C, 78.65; H, 3.06; N, 12.80.

*2.2.7. Synthesis of 1-[(E)-2-{4-[(E)-2-(2-hydroxynaphthalen-1-yl)diazen-1-yl]phenyl}diazen-1-yl]naphthalen-2-ol (**vii**):*

1-[(E)-2-{4-[(E)-2-(2-hydroxynaphthalen-1-yl)diazen-1-yl]phenyl}diazen-1-yl]naphthalen-2-ol (**vii**) was synthesized by diazotization of p-phenylenediamine (PPDA) and then coupling with 2-naphthol. The procedure is as follows: sodium nitrite (3.34 g in 25 mL cold water) was slowly added to PPDA (2.5 g in 10 mL dil. HCl) and the reaction was maintained at 0-5 $^{\circ}$C. After the complete addition of sodium nitrite, the solution was kept for 20 min with constant stirring and maintained at same temperature to yield diazonium salt solution [24]. Then the diazonium salt solution was mixed with cold solution of 2-naphthol (7.2 g in 30 mL of 10% aq. NaOH solution) to yield dark brown product (**vii**) which was filtered to obtain a solid product and it was washed with excess of cold double distilled water to remove the unreacted 2-naphthol. Yield: 90%. Melting point: 118 $^{\circ}$C

FT-IR (cm^{-1}): 1600 (C=C aromatic stretching), 2980 (C-H stretching), 3200-3500 (-OH stretching),

^{1}H NMR: (400 MHz, DMSO-d_6): δ 7.09 (q, J = 2.4 Hz, 2H), 7.11-7.23 (m, 1H), 7.26 (t, J = 6.0 Hz, 1H), 7.76 (d, J = 3.2 Hz, 1H), 7.80 (d, J = 8.8 Hz, 2H), 9.75 (br.s, 1H).

Anal. for $C_{26}H_{18}N_4O_2$: Calc. C, 74.63; H, 4.34; N, 13.39; O, 7.65. Found: C, 74.20; H, 4.20; N, 13.57.

MS (ESI): Calc; 418.44 g/mol for $C_{26}H_{18}N_4O_2$, m/z: 420 (M+1), 278.2 [fragment ion (M+2-(molecular weight of 2-naphthol))].

*2.2.8. Synthesis of ligand 4-({1-[(E)-2-{4-[(E)-2-[2-(3,4-dicyanophenoxy)naphthalen-1-yl]diazen-1-yl]phenyl}diazen-1-yl]naphthalen-2-yl}oxy)benzene-1,2-dicarbonitrile (**viii**):*

Compound **viii** was prepared by using the same procedure employed for the synthesis of compound **ii** but compound **vii** was used instead of compound **i**. The precipitate was washed with

excess water and recrystallized from aq. ethanol and dried over P_2O_5. Yield. 80%. Melting point: 220 °C.

FT-IR (cm^{-1}): 1587(C=C stretching), 2928 (C-H stretching) and 2224 (-CN stretching)

^{1}H-NMR (400 MHz, DMSO-d_6): δ 7.36-7.39 (m, 1H), 7.48 (q, J = 2.4 Hz, 1H), 7.52-7.57 (m, 2H), 7.72 (d, J = 2.4 Hz, 1H), 7.90 (t, J = 2.8 Hz, 2H), 7.93-7.98 (m, 1H), 8.12 (d, J = 8.8 Hz, 2H).

Anal. for $C_{42}H_{22}N_8O_2$: Calc. C, 75.22; H, 3.31; N, 16.31; O, 4.77. Found: C, 75.42; H, 3.18; N, 16.65.

*2.2.9. Preparation of 4-[3'-(3,4-dicyanophenoxy)-3H-spiro[2-benzofuran-3,9'-xanthene]-3-oneoxy]benzene-1,2-dicarbonitrile (**ix**):*

Compound **ix** was prepared by using the same procedure described for compound **ii** but fluorescein was used instead of compound **i**. The precipitate was washed with excess of water and the crude product was recrystallized from aq. ethanol and dried over P_2O_5. Yield: 80%. Melting Point: 122 °C

FTIR (cm^{-1}): 1610 (C=C), 3010 (C-H), 3300-3500 (-OH) and 2226 (-CN).

^{1}HNMR (400 MHz, DMSO-d6): δ 7.24 (d, J = 12.0 Hz, 4H), 7.45 (q, J = 4.0 Hz, 6H), 7.87-7.89 (m, 1H), 7.91-7.99 (m, 6H), 8.11 (d, J = 12.0 Hz, 2H).

Anal. for $C_{37}H_{18}N_4O_4$: Calc. C, 76.28; H, 3.11; N, 9.62; O, 10.9. Found: C, 78.92; H, 4.12; N, 10.50.

MS (ESI): Calc. 583 m/z for $C_{37}H_{18}N_4O_4$: m/z: 585 $(M+2H)^+$.

*2.2.10. Synthesis of 2-(3,4-dicyanophenoxy)-2-methylpropanoic acid (**x**):*

Compound **x** was prepared as explained for compound **ii** by using α-hydroxyisobutyric acid instead of compound **i**. The obtained crude product was purified by 230x400 silica gel chromatography using 9:1 $CHCl_3$/MeOH as eluent. Yield: 70%.

Melting point: 129 °C.

FTIR (cm^{-1}): 1750 (-C=O stretching), 1600 (C=C stretching), 2910 (C-H stretching) and 2218 (-CN stretching).

^{1}H-NMR (400 MHz, DMSO-d6): δ 1.23 (s, 6H), 7.27 (dd, J=1.8, 9.2 Hz, 1H), 7.41 (d, J= 8.0 Hz, 1H), 7.49 (d, J= 1.0 Hz, 1H), 11.2 (br s, 1H).

Anal. for $C_{12}H_{10}N_2O_3$: Calc. C, 62.30; H, 4.38; N, 12.17; O, 20.85. Found: C, 62.47; H, 4.69; N, 12.6.

*2.2.11. Synthesis of 2-[(3,4-dicyanophenyl)sulfanyl]pyridin-1-ium-1-olate (**xi**):*

Compound **xi** was prepared as explained for compound **ii** but 2-mercaptopyridine-N-oxide was employed instead of compound **i**. The reaction product was extracted with ethylacetate and washed with water. The organic layer was separated and dried over P_2O_5. Yield: 70%. Melting point. 176 $^{\circ}$C.

FTIR (cm^{-1}): 1590 (C=C), 2950 (C-H), 2231 (-CN).

^{1}H-NMR (400 MHz, DMSO-d6): δ 6.88 (d, J= 10.0 Hz, 1H), 7.20 (dd, J= 1.4, 8.6 Hz, 1H), 7.44 (d, J= 1.2 Hz, 1H), 7.80 (d, J=7.0 Hz, 1H), 8.10 (dd, J= 1.2, 9.8 Hz, 1H), 8.40 (d, J=7.0 Hz, 1H).

Anal. for $C_{13}H_8N_3OS$: Calc. C, 61.4; H, 3.17; N, 16.5; O, 6.29; S, 12.6. Found: C, 61.72; H, 34.4; N, 16.55; S, 12.43.

2.3. Synthesis of substituted phthalocyanines:

*2.3.1. Synthesis of Zinc tetra 3-[(4-nitrophenyl)amino]-1-phenylpropan-1-one-3-phenoxy phthalocyanine **[Pc 1]**:*

Compound **ii** (1.5 g, 0.003 M) and $ZnCl_2$ (0.104 g (0.0008 M) were transferred into a flask containing 10 ml of 1-pentanol and 0.1mL of DBU [25]. The reaction mixture was refluxed at ~140 $^{\circ}$C with constant stirring for 24 h. Upon reaction completion, the mixture was allowed to attain the room temperature and methanol was added to the crude product to yield dark green product. The precipitate was then filtered and successively washed with methanol and acetone. The product is then dried over P_2O_5. Yield: 75%.

FTIR (cm^{-1}): 760, 872, 980, 1090, 1111 (phthalocyanine skeletal vibrations) and 3360 (-NH stretching).

UV-Visible, nm (log ε):356 (5.24), 700(5.12).

Anal. For $C_{116}H_{80}N_{16}O_{16}Zn$: Calc. C, 68.99; H, 3.99; N, 11.10; O, 12.68; Zn,3.24. Found: C, 70.18; H, 3.85; N, 11.40; Zn, 3.04.

*2.3.2. Synthesis of tetra 3-amino-propan-1-one-1,3-bis(phenoxy) zinc phthalocyanine polymer **[Pc 2]**:*

Tetra 3-amino-propan-1-one-1,3-bis(phenoxy) zinc phthalocyanine polymer **[Pc 2]** was prepared using the procedure for **Pc-1** but using compound **iv** was employed instead of **ii**. Compounds with two phthalonitrile units will produce the symmetrical metallophthalocyanine polymers as in the literature [26-28]. Yield: 75%.

FTIR (cm^{-1}): 765, 880, 990, 1085, 1115 (phthalocyanine skeletal vibrations) and 2220 (weak, -CN stretching for peripheral Pcs)

UV-Visible, nm (log ε**)**: 266 (5.23), 678 (5.10)

Anal. For: $C_{92}H_{68}N_{12}O_{12}Zn$: Calc. C, 69.10; H, 4.29; N, 10.51; O, 12.01; Zn, 4.09. Found: C, 69.40; H, 4.39; N, 10.31; Zn, 3.89.

*2.3.3. Synthesis of Zinc tetra 4-(4-(p-tolyimino)methyl)phenoxy phthalocyanine **[Pc-3]**:*

Pc-3 was obtained using the same synthetic route employed for **Pc–1** but compound **vi** was used instead of **ii**. Yield: 75%.

FTIR (cm^{-1}): 748, 878, 969, 1071 and 1109 (phthalocyanine skeletal vibrations), 1610 (C=N stretching) 2920 (-CH stretching).

UV-Visible, nm (log ε): 355(5.16), 681(4.95).

Anal. For $C_{88}H_{60}N_{12}O_4Zn$: Calc. C, 74.78; H, 4.27; N, 11.8; O, 4.52; Zn, 4.62. Found: C, 76.80; H, 5.34; N, 12.4; Zn, 4.8.

MS (ESI): Calc; 1414.88 g/mol for $C_{88}H_{60}N_{12}O_4Zn$, m/z: 1415.93 (M-1).

*2.3.4. Preparation of substituted tetra (E)-(naphthalen-1-yl)({4-[(E)-2-(naphthalen-1-yl)diazen-1-yl]phenyl})diazene-bis(oxy) zinc phthalocyanine polymer **[Pc 4]:***

Tetra (E)-(naphthalen-1-yl)({4-[(E)-2-(naphthalen-1-yl)diazen-1-yl]phenyl})diazene-bis(oxy) zinc phthalocyanine polymer **[Pc 4]** was synthesised as described **Pc-1** but compound **viii** was used instead of **ii**. Yield: 70%.

FT-IR (cm^{-1}): 759, 893, 964, 1104, 1133 (phthalocyanine skeletal vibrations) and 2215 (-CN stretching)

UV-Visible, nm (log ε): 356(5.19), 683(4.77).

Anal. For: $C_{136}H_{80}N_{24}O_8Zn$: Calc. C, 72.80; H, 3.59; N, 14.98; O, 5.70; Zn, 2.92. Found: C, 73.15; H, 3.74; N, 14.80; Zn, 2.72.

2.3.5. Preparation of tetra 3H-spiro[2-benzofuran-3,9'-xanthene]-3-one-3',6'-bis(oxy) zinc phthalocyanine polymer ***[Pc 5]:***

Pc-5 was synthesized as described for **Pc-1** but compound **ix** was used instead of **ii**. Yield: 70%.
FTIR (cm^{-1}): 770, 898, 960, 1110, 1131 (phthalocyanine skeletal vibrations) and 2226 (-CN stretching).
UV-Visible, nm (log ε): 288 (4.44), 692 (4.95).

Anal. For: $C_{116}H_{64}N_8O_{16}Zn$: Calc. C, 73.67; H, 3.41; N, 5.92; O, 13.54; Zn, 3.46. Found: C, 73.55; H, 3.53; N, 5.80; Zn, 3.58.

2.3.6. Synthesis of Zinc tetra 2-methylpropanoic acid-2-oxy phthalocyanine ***[Pc 6]:***

Pc-6 was synthesized as described for **Pc-1** but compound **x** was used instead of compound **ii**. Yield: 65%.
FTIR (cm^{-1}): 745, 885, 958, 1094, 1129 (phthalocyanine skeletal vibrations) and 1765(C=O stretching of -COOH) and 3110-3450 cm^{-1} (-OH stretching of -COOH).
UV-Visible, nm (log ε): 290(5.00), 693(4.86).

Anal. for $C_{48}H_{40}N_8O_{12}Zn$: Calc. C, 58.40; H, 4.0; N, 11.35; O, 19.4; Zn, 6.62. Found: C, 58.71; H, 3.70; N, 12.56; Zn, 7.05.
MS (ESI): Calc; 986.37 g/mol for $C_{48}H_{40}N_8O_{12}Zn$, m/z: 985.5(M+1).

*2.3.7. Synthesis of Aluminium chloro tetra pyridin-1-ium-1-olate-2-sulfanyl phthalocyanine [**Pc 7]:***

Pc-7 was synthesized as described for **Pc-1** but compound **xi** and $AlCl_3$ were used instead of compound **ii** and $ZnCl_2$. Yield: 65%.

FTIR (cm^{-1}): 755, 892, 970, 1005, 1125 (phthalocyanine skeletal vibrations)
UV-Visible, nm (log ε): 331 (5.04), 687(5.06).

Anal. for $C_{52}H_{32}N_{12}O_4S_4$: Calc. C, 57.80; H, 2.96; N, 20.75; S, 11.88; Cl, 3.28; Al, 2.50. Found: C, 58.22; H, 2.50; N, 20.8; S, 12.21

3. Results and discussions

3.1. Synthesis and characterization of the Pc complexes

The synthesis of the ligands and substituted zinc and aluminium phthalocyanine complexes and polymers were carried out as shown in **Table 1** and **Scheme 1**. The first step involves the preparation of hydroxyl or sulfanyl precursors for all the Pcs. The second step involves the base catalyzed nucleophilic aromatic nitro displacement of 4-nitrophthalonitrile with hydroxyl or sulfanyl group containing precursors to yield phthalonitrile/bisphthalonitrile ligands [29,30]. The phthalonitrile ligands undergo cyclotetramerization to form the symmetrical substituted phthalocyanine complexes, whereas bisphthalonitrile forms polymeric phthalocyanines. In the first step of polymerization, four molecules of corresponding bisphthalonitrile ligand reacts to give substituted octacyanophthalocyanine. Then the peripheral cyano groups of phthalocyanine units interact at high temperature to yield fused ring structure joined at the sides to form ladder polymeric Pcs. This type of conjugated ladder polymer has advantages over single stranded conjugated polymer in terms of chemical resistance, thermal stability, mechanical strength and greater molecular and structural order [31].

The reactions were monitored by TLC and the synthesized ligands were purified and characterized with, FT-IR, NMR, mass spectroscopy and melting point (NMR and mass spectral data are provided in supplementary information). The phthalocyanine complexes and polymers were successfully purified to afford blue to green product with solubility in DMSO, DMF and concentrated H_2SO_4. The polymeric Pc's are less soluble compared to the monomeric Pc's.

3.1.1. FTIR Characterization:

FT-IR spectra for all the synthesised ligands and phthalocyanine complexes were recorded in the region 400 to 4000 cm^{-1}. The FTIR spectra of compounds **i** to **xi** are shown in **Fig 1**, all the compounds showed vibrational band at 1540-1620 cm^{-1} which corresponnd to C=C

stretch and 2870-3020 cm^{-1} corresponding to C-H stretch. Compounds **i**, **iii**, **v** and **vii** showed broad peaks at 3100-3450 cm^{-1} which is assigned to -OH.

In addition, compound **i-iv** showed vibration band at 1650-1700 cm^{-1} corresponding to C=O, **i** and **ii** showed peak at 3340-3350 cm^{-1} which corresponds to –NH (secondary amine) and compounds **iii** and **iv** showed bands at 3300-3330 cm^{-1} corresponding to $-NH_2$. A peak was observed for compound **v** at 1600 cm^{-1} which can be assigned to C=N. The IR spectra for compound **vi** exhibited vibrational bands at 1610 and 1475 cm^{-1} corresponding to C-C ring skeletal stretch–vibrations and the 720 cm^{-1} band to -CH out of plane bending vibrations. Compound **ix** showed peak at 1750 cm^{-1} accountable to the C=O peak and compound **x** at 1750 cm^{-1} for C=O of the carboxylic acid with broad peak at 3110-3450 cm^{-1} for –OH of the carboxylic acid. Compound **xi** showed peak at 1270 cm^{-1} may be due to the NO of pyridine-N-oxide [32].

Ligands **ii**, **iv**, **vi**, **viii**, **ix**, **x** and **xi** showed sharp peak at 2200-2290 cm^{-1} corresponding to –CN group. The appearance of -CN group and disappearance of –OH or –SH peak confirms the formation of the conjugated phthalonitriles . In addition to TLC, IR was useful in monitoring the completion of the formation of cyano ligands from their counter hydroxy ligands by monitoring the appearance of cyano group peak at ~2250 cm^{-1} with the complete disappearance of the hydroxy or sulfanyl group at ~3300 cm^{-1} or 2550 cm^{-1}. All the phthalocyanine complexes showed peaks at 745-760, 875-895, 965-990, 1004-1110 and 1111-1135 cm^{-1} which can be assigned to the phthalocyanine skeletal vibrations [33]. Additionally, the IR spectra of Pcs showed disappearance of –CN peak in **Pc-1**, **Pc-3**, **Pc-6** and **Pc-7** indicating the consumption of cyano groups to form phthalocyanine macrocycle. Whereas in polymeric Pc's (**Pc-2**, **Pc-4** and **Pc-5**), though the intensity of the cyano peak at 2200-2290 cm^{-1} was decreased but did not disappear completely due to the terminal –CN peak of polymeric Pc's. The peaks of the polymer were slightly lesser in intensity and broader in nature as compared to the monomeric Pcs.

3.1.2. UV-Vis spectra:

The UV Visible spectra for all the Pcs were recorded by dissolving 1mg dry phthalocyanine in 5 mL DMSO. The UV-Vis spectra were recorded in the range of 250 to 900 nm at a scan rate of 240 nm min^{-1}.

Figure ES-12 shows the absorption spectra of the Pc's. All the synthesized Pc's showed absorption peaks at 250-280, 335-360, 414-450, 620-650 (shoulder peak) and 685-705 nm, Table 1. The peak observed in the UV region at 335-360 nm correspond to B-band and the peak observed at 620-650 nm can be accounted for the oligomer and dimeric forms of the phthalocyanine macrocycle and the intense Q-band was observed at 685-705 nm [34]. The absorption spectra of **Pc-4**, **Pc-5**, **Pc-6** and **Pc-7** showed split Q-band. The splitting of the Q-band in **Pc-6** and **Pc-7** suggests aggregation of the macrocycle whereas the splitting in case of **Pc-4** and **Pc-5** may be due to the polymeric nature of the macrocycle. The deep intense blue/green colour of the phthalocyanines is due to the peak at 670-700 nm which arises because of the π-π* transitions of the conjugated macrocycle [35].

3.1.3. TGA studies:

TGA studies provide information about the thermal stability and decomposition behaviour of the synthesized phthalocyanine compounds. The thermogram for the thermal degradation of the phthalocyanines is shown in **Fig. 2**.

It was observed from the thermograms that the monomeric Pcs are stable up to 300 °C and then starts to degrade in air atmosphere in the region of 350–490 °C which leads to the rapid loss of weight corresponding to the degradation of core structure of phthalocyanine molecule. Whereas, the polymeric Pcs were found to be stable up to 500 °C and then the polymeric molecule starts to degrade in air atmosphere in the region of 520–650 °C. **Pc-4** shows higher thermal stability than other two polymeric Pcs due to the extended conjugation and delocalization of π-electrons. The stable TGA curve after 520 °C corresponds to the respective metal oxide formed after complete degradation of the Pcs. The weight remaining after 490°C in the TG curve is theoretically equivalent to metal oxide of the sample taken for TGA analysis.

***3.1.4. NMR and Mass spectra*:**

NMR and mass spectroscopy gives the information about the structural and molecular mass of the compounds. In particular ^{1}H-NMR gives the information about the chemical environment of the protons present in the compound. The number of non-equivalent protons are equal to the number of peaks in the NMR spectra. ^{1}H-NMR spectra was recorded for all the synthesized compounds (i-xi) in different deuterated solvents, such as for compound (i) in deuterated methanol (methanol-d_4), compound (ii) in CDCl3 and compounds (iii-xi) in deuterated DMSO

(DMSO-d6). The synthesized compounds are having different types of protons like aromatic protons, aliphatic protons, -OH, and amine groups. The aromatic protons show peaks around 6-8 δ, aliphatic protons (-CH_3 at 0.9-1.5 δ, -CH_2 at 1.2-1.8 δ and –CH at 1.5-2.1 δ) at 1-2.2 δ, -OH at 3-10 δ and primary and secondary amines at 5-6.5 δ. All the precursor compounds exhibited broad singlet peak for –OH and –SH group proton, whereas this peak disappeared in their corresponding ligands confirming the formation of respective ligands. In addition, the ^{1}H-NMR peaks obtained for different ligands are well matching with the theoretical data for the proposed structures.

Mass spectra gives the information about the molecular weight and the fragmentation of the compounds. The synthesized ligands showed (M^+ or M^-) molecular ion peaks in mass spectra which are well coinciding with the theoretical molecular weight of the compounds. Some ligands showed fragment ion peaks which are responsible for the detachment of one part of the molecule from the ligand. The mass spectra of Pc-3 displayed peak at 1415.9 corresponding to M^{-1} molecular ion, Pc-6 showed peak at 985.5 corresponding to M^{+1} molecular ion. The NMR and mass spectra of the precursors, ligands and complexes suggests the successful formation of pure desired compounds.

3.2. Photophysicochemical Parameters

The fluorescence (Φ_F) and singlet oxygen (Φ_Δ) quantum yields of the Pc complexes were determined using comparative methods reported in the literatures [36-38]. Unsubstituted ZnPc dissolved in DMSO was used as a standard (Φ_F =0.20 [37], and Φ_Δ = 0.67 [38] in DMSO using DPBF as a quencher).

3.2.1. Fluorescence (Φ_F) quantum yields and lifetimes (τ_F)

Figure 3 (using **Pc-2** and **Pc-6** as examples) shows the normalised absorption, emission and excitation spectra and **figure ES 11** (for all the Pc complexes) shows the ground state electronic absorption, emission and excitation spectra of Pc complexes in DMSO. The absorption and excitation spectra were similar and mirror images of the emission spectra for **Pc–2**. This applied to all non-aggregated complexes. **Pc–6** and other aggregated complexes showed a slightly different behaviour with absorption spectra different from the excitation spectra due to the presence of aggregates in the absorption spectra. Aggregates do not fluoresce. Aggregation in

Pc's is often judged by the broadening or split in the Q band with the high energy band being due to the so called "H" aggregates [39].

The fluorescence quantum yields and lifetimes of the Pc complexes were measured in DMSO with **Pc–5** accounting for the highest Φ_F value (0.16) while **Pc–4** and **Pc–6** accounted for the least Φ_F value (0.02), **Table 2**. Low Φ_F values are due to aggregation. A typical fluorescence decay curve is shown in **Figure 4** for Pc complexes (using **Pc–5** as an example). A single fluorescence lifetime was observed for all the Pc complexes. Additionally, the fluorescence quantum yields of the Pc complexes afforded corresponding fluorescence lifetimes which is expected since there is a direct correlation between the former and latter except for **Pc–6** which showed a decrease in its fluorescence lifetime despite the relatively high fluorescence quantum yield, it afforded.

3.2.2. Singlet Oxygen Quantum Yield

The singlet oxygen quantum yields of the Pc complexes were determined using photochemical method involving DPBF as singlet oxygen quencher which was spectroscopically monitored from 0 s to 120 s at ~417 nm. Concentrations of Pc complexes for the determination of singlet oxygen quantum yield are as follows, Pc–1 (8.12×10^{-6} M), Pc–2 (7.95×10^{-6} M), Pc–3 (1.15×10^{-5} M), Pc–4 (2.02×10^{-5} M), Pc–5 (1.11×10^{-5} M), Pc–6 (1.35×10^{-5} M) and Pc–7 (1.06×10^{-5} M). The characteristic change in absorbance profile of DPBF in the presence of PS is shown in **Figure 5** (using **Pc–2** as an example). A gradual decrease in the absorbance of DPBF was observed suggesting the production of singlet oxygen. There was no change in the intensity of the Q band for all the Pc complexes on exposure to illumination inferring the photostability of the Pc complexes. **Pc–1**, **Pc–6** and **Pc–7** showed a relatively low singlet oxygen quantum yields which might be attributed to plausible aggregation as earlier shown in their UV–vis spectra (**Table 2)**.

3.3 Cell studies

Cell culture and treatment

The *in vitro* dark cytotoxicity and photodynamic therapy activities of the photosensitizers (PS) were performed as described in the literature [25, 40]. Details of the protocol are provided in the supporting information.

The cell viability represents the fraction of active cells after PS treatment and incubation for 24 h often expressed as a normalized percentage. Prior to PDT studies, the *in vitro* dark cytotoxicity of the PS were carried out in the absence of illumination to ascertain their applicability for PDT since dark cytotoxicity of PS is undesirable in PDT due to plausible lack of selectivity and specificity towards tumorigenic cells as opposed to healthy cells.

3.3.1. In vitro dark cytotoxicity

Figure 6A and 6B shows the histograms for the *in vitro* dark cytotoxicity and PDT activities of PS against MCF–7 cells (using **Pc–5** as an example for the gradient PS concentrations). All the PS accounted for ≥81% viable cells within the concentration range of 5–80 μg/mL inferring minimal *in vitro* dark cytotoxicity which is a good indication for PS meant for PDT application, **Figure 6A and 6B**. The overall confluence of the cells in the presence of PS were relatively unaltered as compared to the control cells, Figure not shown.

The Synergy 2 multi–mode microplate reader was used to assess the cellular uptake of the PS [41]. From **Figure 7** (using **Pc-3** as an example), it can be observed that the cellular uptake of the PS was concentration dependent due to the increase in the cellular uptake as the PS concentration increases. There was steady cellular uptake of the PS as the concentration increases. The efficient steady uptake of the PS by the cell is advantageous for PDT due to the availability of the unchanged PS in the cells which will inevitably elicit pharmacological response on exposure to light.

3.3.2. In vitro photodynamic therapy evaluation

The *in vitro* PDT evaluation of the PS was carried out at the same concentrations and experimental conditions as the *in vitro* dark cytotoxicity studies except for irradiation of the incubated cells having the PS at 680 nm and laser beam dosimetry of 85 $J.cm^{-2}$, respectively.

Significant decrease in the cell viability of the cells having PS exposed to light was observed in comparison to the ones without irradiation. PDT activity increased moderately with PS concentration increases, Fig. 6A. Of importance is the high PDT activity observed for the **Pcs 5–7** with less than 50% viable cells as compared **Pcs 1–4** which showed greater than 50% viable cells across all the tested concentrations (5–80 μg/mL) using 80 μg/mL as an example for all the complexes, **Figure 6C**. **Pcs 6** and **7** showed the highest PDT effect with 57% cell death while **Pc**

3 accounted for 33% cell death. It is important to note that the latter showed the highest singlet oxygen quantum yield (**Table 2**) as compared to the former or other Pcs considered in this study but afforded the least PDT activity, **Figure 6C**. It has been reported that the PDT activity of PS is dependent on factors such as cell type, cellular uptake and localization [42]. However, the PS with high singlet oxygen quantum yields could have suffered from low cellular uptake and localization as compared to the others with low singlet oxygen quantum yields which showed high PDT since they differ greatly on their ring substituents. The overall confluence of the cellular micrographs in the presence of PS were significantly altered as compared to the control cells evidenced by the photo–micrographs, **Figure 8** (using Pcs **1** and **2** as examples). From the photo–micrographs, it can be deduced that the confluence of the cells having the PS were low as compared to the control cells which is a good indication for the PDT activity of the PS.

4. Conclusion:

The present work demonstrates the successful synthesis of novel Zn and Al phthalocyanine derivatives in pure state. All the Pcs showed significant PDT activity compared to the *in vitro* dark cytotoxicity behavior, but **Pc–1** to **Pc–4** showed ≥50% viable cells within the tested concentration range of 5–80 μg/mL. The remarkable PDT activity was shown by **Pc–5** to **Pc–7** with **Pc–5** showing less than 50% viable cells at 80 μg/mL, while **Pc–6** and **Pc–7** achieved the same efficacy at 40 μg/mL and 80 μg/mL. Though, **Pc–6** and **Pc–7** exhibited low singlet oxygen quantum yields in DMSO plausibly due to aggregation, but showed higher PDT activity compared to the other PS (**Pc–1** to **Pc–5**) with larger Φ_Δ values. This phenomenon could be ascribed to better interaction of the PS (**Pc–6** and **Pc–7**) in slightly amphiphilic media compared to the lipophilic ones. On visualization of the bright field fluorescence micrographs of the placebo cells and treated cells (cells having PS), significant alteration in the overall confluence of the treated cells was observed compared to the control cells. The observed spaces in the treated cells could be attributed to the cytocidal activity of the PS against the MCF–7 cells on exposure to light.

Acknowledgements:

This work was supported by the Department of Science and Technology (DST) Innovation and National Research Foundation (NRF), South Africa through DST/NRF South African Research Chairs Initiative for Professor of Medicinal Chemistry and Nanotechnology

(UID 62620), DST-SERB, grant No. SERB/ F/9388/ 2016-17, CSIR EMR-II grant, VGST K-FIST support (GRD No.555), DST-FIST grant and Directorate of Minorities, Karnataka Government (GOKDOM) is also acknowledged.

References:

[1] Leznoff CC., Lever ABP. Phthalocyanines: properties and applications vols. 1–4., New York: VCH Publishers; 1996. 1989, 1992, 1993.

[2] Erk P. Hengelsberg, H., Kadish KM., Smith KM., Guilard, R. Eds,; The Porphyrin Handbook Academic Press: Volume 19, 2003; p 105-149.

[3] Schramm CJ, Scaringe RP, Stojakovic DR, Hoffman BM, Ibers JA, Marks TJ. Chemical, Spectral, Structural, and Charge Transport Properties of the "Molecular Metals" Produced by Iodination of Nickel Phthalocyanine. J Am Chem Soc 1980;102:6702-13.

[4] Zekeriya B, Çakır V, Koca A, Kantekin H. Synthesis, electrochemical, in-situ spectroelectrochemical and in-situ electrocolorimetric characterization of non-peripheral tetrasubstitute metal-free and metallophthalocyanines. Dye Pigment 2011;89:49-55.

[5] Karaoğlu HRP, Koca A, Koçak MB. Synthesis, Electrochemical and Spectroelectrochemical Characterization of Novel Soluble Phthalocyanines Bearing Chloro and Quaternizable Bulky Substituents on Peripheral Positions. Dye Pigment 2012;92:1005-17.

[6] Özçeşmeci I. Synthesis and Fluorescence Properties of Phthalocyanines with Dibromo- and Tribromo-Phenoxy Functionalities. Synth Met 2013;176:128– 33.

[7] Edrissi M, Nasernejad B, Sayedi B. Novel Method for the Preparation of Copper Phthalocyanin Blue Nanoparticles in an Electrochemical Cell Irradiated by Microwave. Int J Eng Trans B Appl 2007;20:257-62.

[8] Zhang XF, Guo W. Imidazole Functionalized Magnesium Phthalocyanine Photosensitizer:

Modified Photophysics, Singlet Oxygen Generation and Photooxidation Mechanism. J Phys Chem A 2012;116:7651-57.

[9] DeRosa MC, Crutchley RJ. Photosensitized Singlet Oxygen and Its Applications. Coord Chem Rev 2002;233-234:351-71.

[10] Ishii K. Functional Singlet Oxygen Generators Based on Phthalocyanines. Coord Chem Rev 2012;256:1556– 68.

[11] Di Mascio P, Kaiser SP, Devasagayam TPA, Sies, H. Biological Significance of Active Oxygen Species: In Vitro Studies on Singlet Oxygen-Induced DNA Damage and on the Singlet Oxygen Quenching Ability of Carotenoids, Tocopherols and Thiols. Advances in Experimental Medicine and Biology 1991;283:71–77.

[12] Allen C.M, Langlois R, Sharman WM, La Madeleine C, Van Lier JE. Photodynamic Properties of Amphiphilic Derivatives of Aluminum Tetrasulfophthalocyanine. Photochem Photobiol 2002;76:208-16.

[13] Aliosman M, Göksel V, Mantareva I, Stoineva M, Durmuş. Tyrosine conjugated zinc(II) phthalocyanine for photodynamic therapy: Synthesis and photophysicochemical properties, J Photochem Photobiol A Chem 2017;334:101-106.

[14] Topal SZ, Ün ŞŞ, Bretonnière Y, Kostakoğlu ST. New designed naphthalimide-phthalocyanine pentads: Synthesis, photophysical and photochemical properties in DMSO and room temperature ionic liquids. J Photochem Photobiol A Chem 2017;332:562-70.

[15] Sharman WM, Allen CM, Van Lier JE. Photodynamic Therapeutics: Basic Principles and Clinical Applications. Drug Discovery Today 1999;4:507-17.

[16] Mehraban N, Freeman H S. Developments in PDT Sensitizers for Increased Selectivity and Singlet Oxygen Production. Materials 2015;8:4421-56.

[17] Fernandez JM, Bilgin MD, Grossweiner LI. Singlet Oxygen Generation by Photodynamic Agents. J. Photochem. Photobiol. B Biol. 1997;37:131- 40.

[18] Matshitse R, Nwaji N, Mananga M, Prinsloo E, Nyokong T. Effect of number of positive charges on the photophysical and photodynamic therapy activities of quarternary benzothiazole substituted zinc phthalocyanine. J Photochem Photobiol A Chem 2018;367:253-260.

[19] Kim HS, Muthukumar P, Ku KS, Son YA. Synthesis and Characterization of Water-Soluble Phthalocyanine Copper(II) Complex and Its Coloration on Acrylic Fibers. Fibers Polym. 2015;16:2552-57.

[20] Oluwole DO, Britton J, Mashazi P, Nyokong T. Synthesis and Photophysical Properties of Nanocomposites of Aluminum Tetrasulfonated Phthalocyanine Covalently Linked to Glutathione Capped CdTe/CdS/ZnS Quantum Dots. Synth Met 2015;205:212–21.

[21] Oluwole DO, Prinsloo E, Nyokong, T. Photophysicochemical properties of nanoconjugates of zinc(II) 2(3)–mono–2– (4–oxy)phenoxy)acetic acid phthalocyanine with cysteamine capped silver and silver–gold nanoparticles. Polyhedron 2016;119:434-44.

[22] Goswami SV, Thorat PB, Chakrawar AV, Bhusare SR. A mild and efficient one-pot synthesis of β-amino carbonyl compounds via Mannich reaction under ambient temperature condition. Mol Divers 2013;17:33- 40.

[23] Vijaykumar BN, Uddhav N, Shaik AK. An Eco-Friendly Protocol for Synthesis of β-aminoketones via Mannich Reaction Using Citric Acid: A Biodegradable Catalyst, IOSR-JAC 2014;7:86-89.

[24] Zarei A, Hajipour AR, Khazdooz L, Mirjalili BF, Najafi A. Chermahini. Rapid and efficient diazotization and diazo coupling reactions on silica sulfuric acid under solvent-free conditions, Dye Pigment 2009;81:240–44.

[25] Wöhrle D, Schnurpfeil G, Knothe G. Efficient Synthesis of Phthalocyanines and Related Macrocyclic Compounds in the Presence of Organic Bases. Dye Pigment 1992;18:91-02.

[26] Guo M, Yan X, Kwon Y, Hayakawa, Kakimoto MA, Goodson T, Iii. High Frequency Dielectric Response in a Branched Phthalocyanine, J Am Chem Soc 2006;128:14820-21

[27] Li LS, Li ADQ. Probing surface electronic potentials and photovoltaic effects of self-assembled multilayers of metal phthalocyanine and oligomeric viologen on conductive substrates. J Phys Chem B 2001;105:10022-28.

[28] Meng F, Zhao R, Xu M, Zhan Y, Lei Y, Zhong J, Liu X. Fe–phthalocyanine oligomer/Fe3O4 nano-hybrid particles and their effect on the properties of polyarylene ether nitriles magnetic nanocomposites, Colloids Surfaces A Physicochem Eng Asp 2011;375:245-51.

[29] Wang H, Wang J, Guo H, Chen X, Yu X, Ma Y, et al. A novel high temperature vinylpyridine-based phthalonitrile polymer with a low melting point and good mechanical properties. Polym Chem 2018;9:976–83.

[30] Smirnov A V, Abramov IG, Plakhtinskii V V, Krasovskaya GG. 4-(1-Benzotriazolyl)-5-nitrophthalonitrile as a highly active substrate in aromatic nucleophilic substitution reactions. Mendeleev Commun 2002;12:72–74.

[31] Lee J, Kalin AJ, Yuan T, Al-Hashimi M, Fang L. Fully conjugated ladder polymers, Chem Sci 2017;8:2503- 21

[32] Kumar M, Srivastava M, Yadav RA. Vibrational Studies of Benzene, Pyridine, Pyridine-N-Oxide and Their Cations. Spectrochim Acta - Part A Mol Biomol Spectrosc 2013;111:242–51.

[33] Manjunatha N, Imadadulla M, Lokesh KS, Venugopala Reddy KR. Synthesis and

electropolymerization of tetra-[β-(2-benzimidazole)] and tetra-[β-(2-(1-(4-aminophenyl))benzimidazole)] embedded cobalt phthalocyanine and their supercapacitance behaviour. Dye Pigment 2018;153:213-24

[34] Imadadulla M, Manjunath N, Lokesh KS. Solvent dependent dispersion behaviour of macrocycle stabilized cobalt nanoparticles and their applications. New J Chem 2018;42:11364-72.

[35] Achar BN, Lokesh KS. Studies on Phthalocyanine Sheet Polymers. J Organomet Chem 2004;689:2601-05.

[36] Fery-Forgues S, Lavabre D. Are Fluorescence Quantum Yields So Tricky to Measure? A Demonstration Using Familiar Stationery Products. J Chem Educ 1999;76:1260-64.

[37] Ogunsipe A, Chen JY, Nyokong T. Photophysical and Photochemical Studies of Zinc(Ii) Phthalocyanine Derivatives-Effects of Substituents and Solvents. New J Chem 2004;28:822-27.

[38] Kuznetsova N, Gretsova NS, Kalmykova EA, Makarova EA, Dashkevich SN, Negrimovskii VM, Kaliya O L, Luk'yanets EA. Relationship between the Photochemical Properties and Structure of Pophyrins and Related Compounds. Russ J Gen Chem 2000;70:133.

[39] Nyokong T, Isago H. The Renaissance in Optical Spectroscopy of Phthalocyanines and Other Tetraazaporphyrins. J Porphyr Phthalocyanines 2004l8:1083-90.

[40] Oluwole DO, Tilbury CM, Prinsloo E, Limson J, Nyokong T. Photophysicochemical properties and in vitro cytotoxicity of zinc tetracarboxyphenoxy phthalocyanine – quantum dot nanocomposites. Polyhedron 2016;106:92–100.

[41] Dube E, Oluwole DO, Prinsloo E, Nyokong T. Gold–chitosan composite with low symmetry zinc phthalocyanine for enhanced singlet oxygen generation and improved photodynamic therapy activity, New J Chem 2018;42:10214-25.

[42] Atilla D, Saydan N, Durmuş M, Gürek AG, Khan T, Rück A, Walt H, Nyokong T. Ahsen V. Synthesis and Photodynamic Potential of Tetra- and Octa-Triethyleneoxysulfonyl Substituted Zinc Phthalocyanines. J Photochem Photobiol A Chem 2007;186:298-307.

Table I: Synthetic scheme for different ligands

Pcs	Synthesis of Ligand	R
Pc-1 M=Zn X=O; Z=H	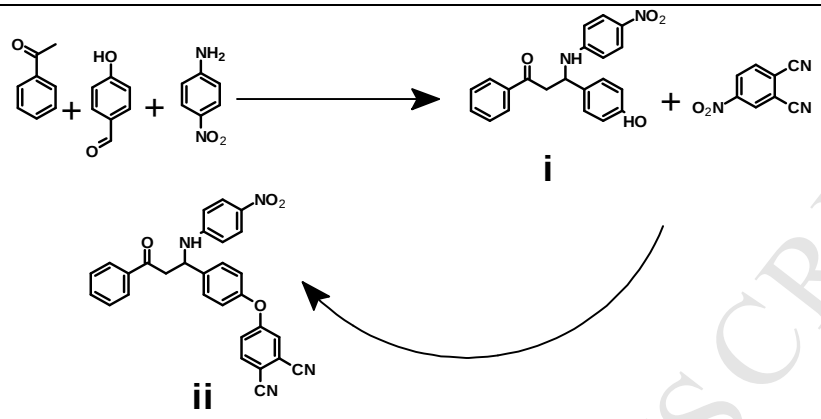	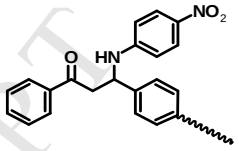
Pc-2 Polymer M=Zn X=O; Z=O	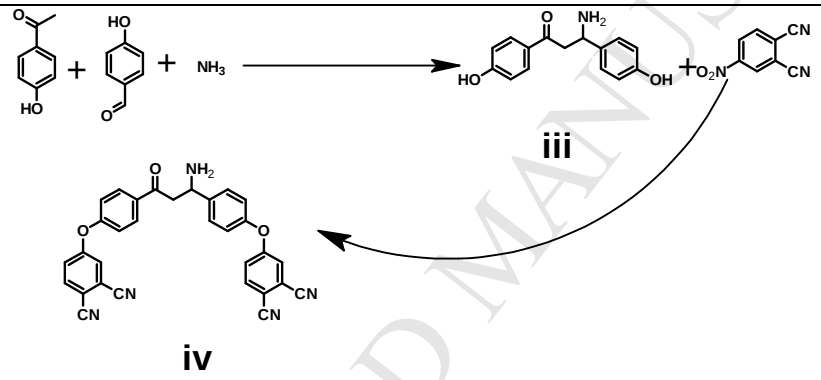	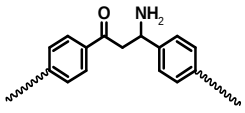
Pc-3 M=Zn X=O; Z=H	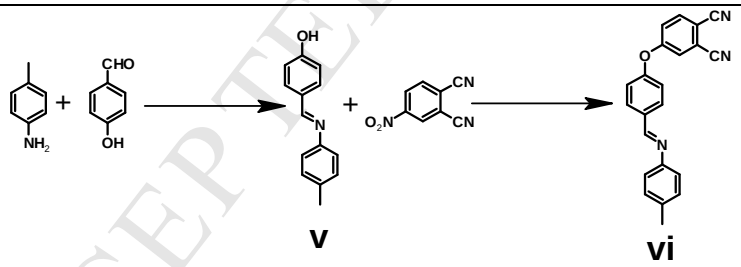	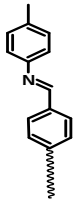

Pc-4 Polymer M=Zn X=O; Z=O	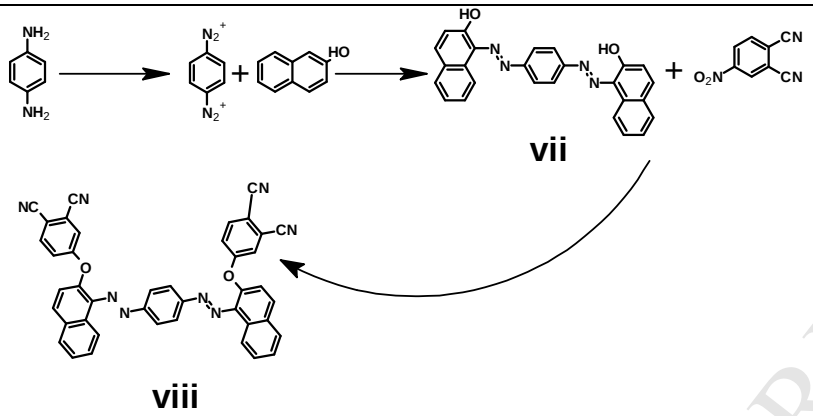 vii viii	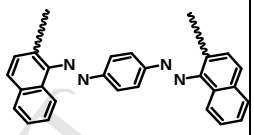
Pc-5 Polymer M=Zn X=O; Z=O	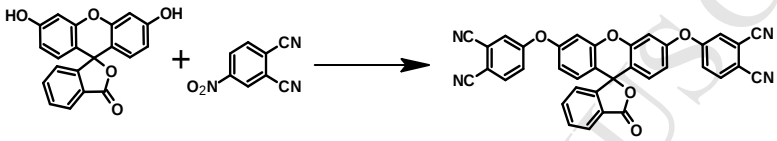 ix	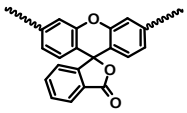
Pc-6 M=Zn X=O; Z=H	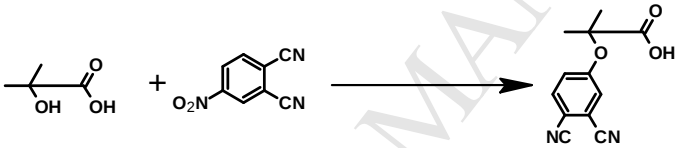 x	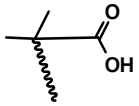
Pc-7 M=$AlCl_3$ X=O; Z=H	 xi	

Table 2: Photophysicochemical parameters for metallophthalocyanines in DMSO

Complexes	$\lambda_{Abs\ (nm)}$	$\lambda_{Ems\ (nm)}$	$\Phi_{F\ (<\pm 0.01)}$	$\tau_{F\ (\pm 0.03)}$	Φ_{Δ}
Pc–1	700	695	0.02	2.40	0.08
Pc–2	680	691	0.06	2.59	0.31
Pc–3	679	692	0.13	2.81	0.49
Pc–4	680	690	0.02	2.34	0.41
Pc–5	681	695	0.16	2.83	0.47
Pc–6*	684	713	0.02	2.40	0.15
Pc–7*	687	697	0.05	2.45	0.10

λ_{Abs} = the highest Q – band intensity was quoted for Pcs 6 and 7

FIGURE CAPTIONS

Scheme 1: Synthetic route for different Phthalocyanines.

Figure 1: FTIR spectra of a) precursor molecules and ligands. (Compounds i to xi) and b) Pcs 1–7.

Figure 2: Thermogravimetric analytical curve for a) Monomeric Pcs and b) Polymeric Pcs.

Figure 3: Ground state electronic absorption, emission and excitation spectra of metallophthalocyanine in DMSO at $\lambda_{excitation}$ = 612 nm (Pc-2) and 616 nm (Pc-6).

Figure 4: Fluorescence lifetime decay curve for Pc complexes in DMSO (using Pc–5 as an example).

Figure 5: Spectra for singlet oxygen quantum yield determination using a photochemical method. The spectra show the degradation of DPBF in the presence of Pc-2 in DMSO.

Figure 6: Histograms for *in vitro* dark cytotoxicity and PDT effect (85 J.cm^{-2}) of (A) various concentrations of Pc-5, (B) Comparative dark toxicity for all complexes at 80 μg/mL and (C) comparative PDT activity (85 J.cm^{-2}) of all complexes 80 μg/mL against MCF–7 cells.

Figure 7: Cellular uptake curves for PS (Pc–3).

Figure 8: Photo–micrographs for *in vitro* PDT effect for the Pc complexes (using control (a) and Pc–7 (b) at 80 μg/mL as examples) against MCF–7 cells. Irradiation dosimetry = 85 J.cm^{-2}. Magnification = 10×, Scale = 200μm.

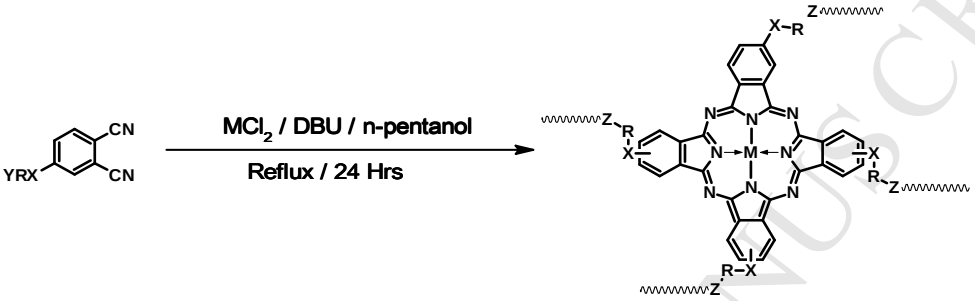

Scheme 1

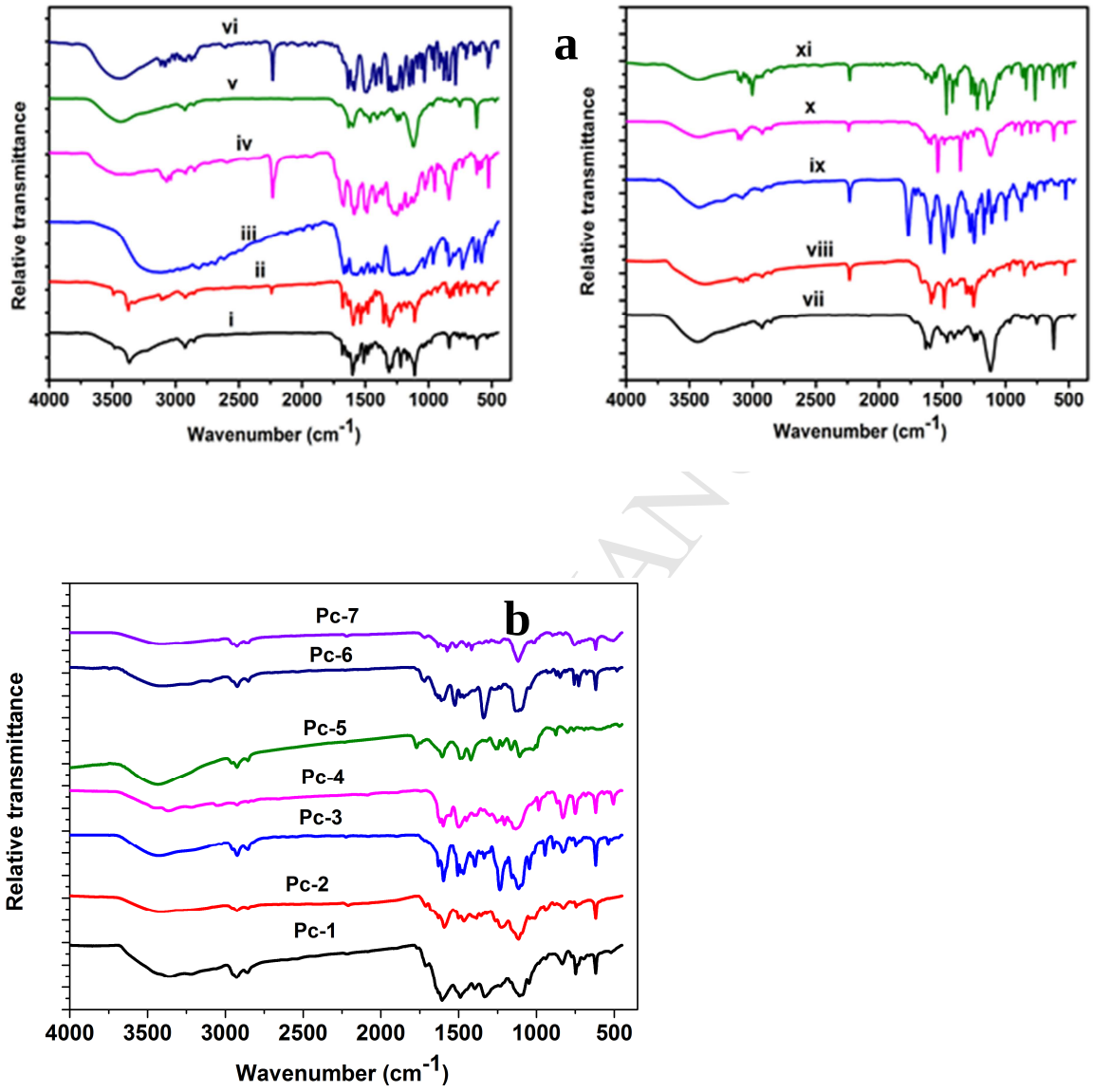
a
vi
v
iv
iii
ii
i
xi
x
ix
viii
vii
Relative transmittance
Wavenumber (cm-1)
4000 3500 3000 2500 2000 1500 1000 500
b
Pc-7
Pc-6
Pc-5
Pc-4
Pc-3
Pc-2
Pc-1

Figure 1

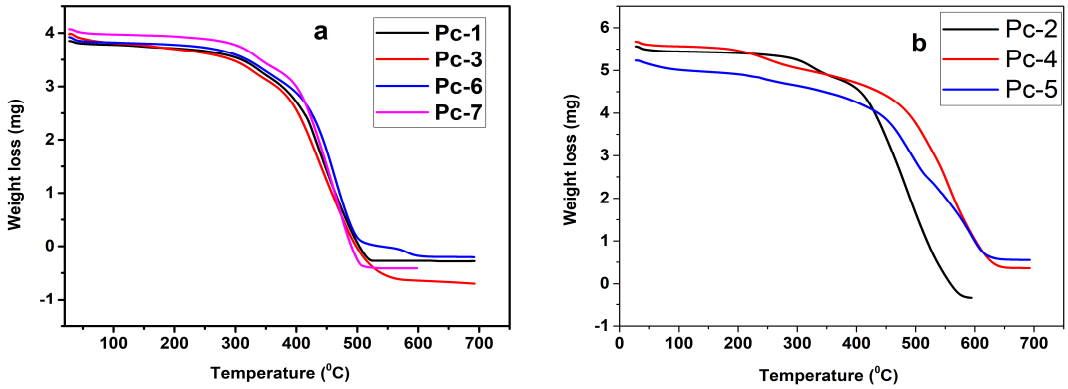

Figure 2

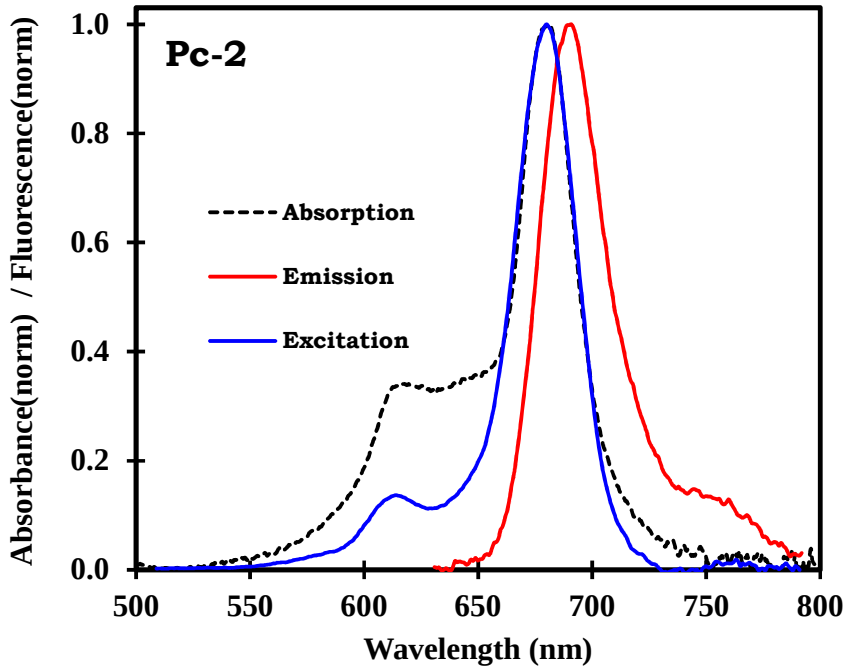
Pc-2
Absorption
Emission
Excitation
Absorbance(norm) / Fluorescence(norm)
Wavelength (nm)
1.0
0.8
0.6
0.4
0.2
0.0
500
550
600
650
700
750
800

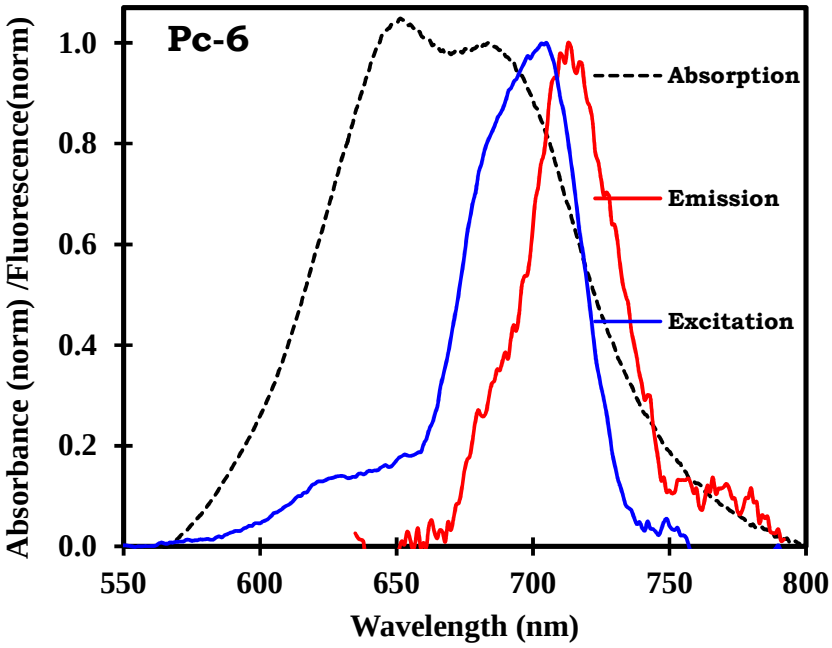
Pc-6
Absorption
Emission
Excitation
Absorbance (norm) /Fluorescence(norm)
Wavelength (nm)
1.0
0.8
0.6
0.4
0.2
0.0
550
600
650
700
750
800

Figure 3

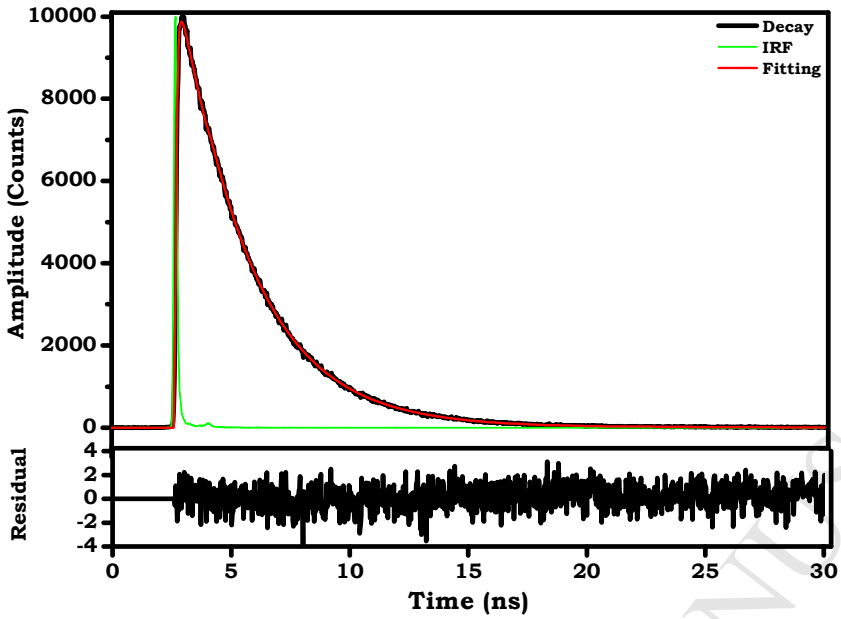

Figure 4

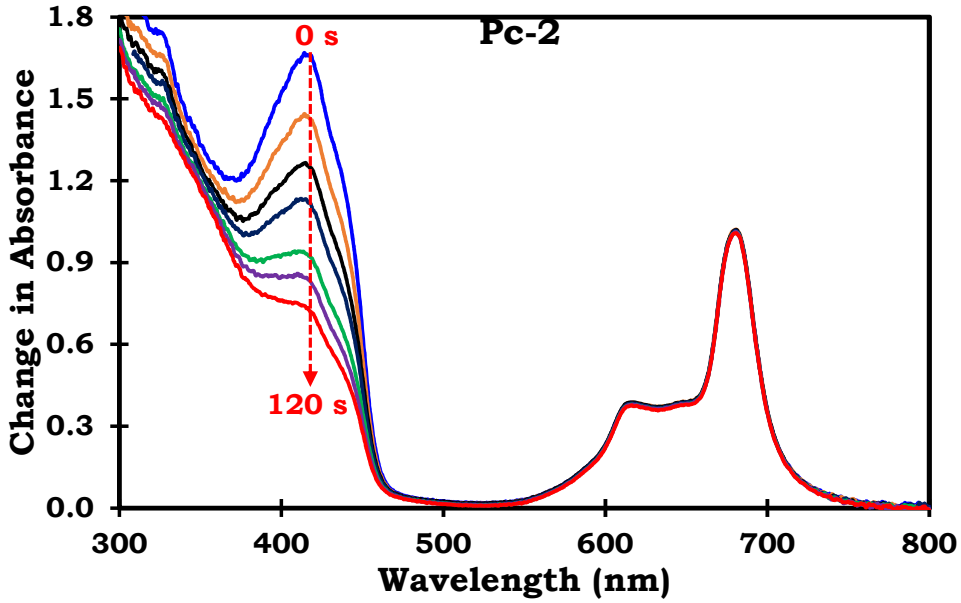

Figure 5

(A)

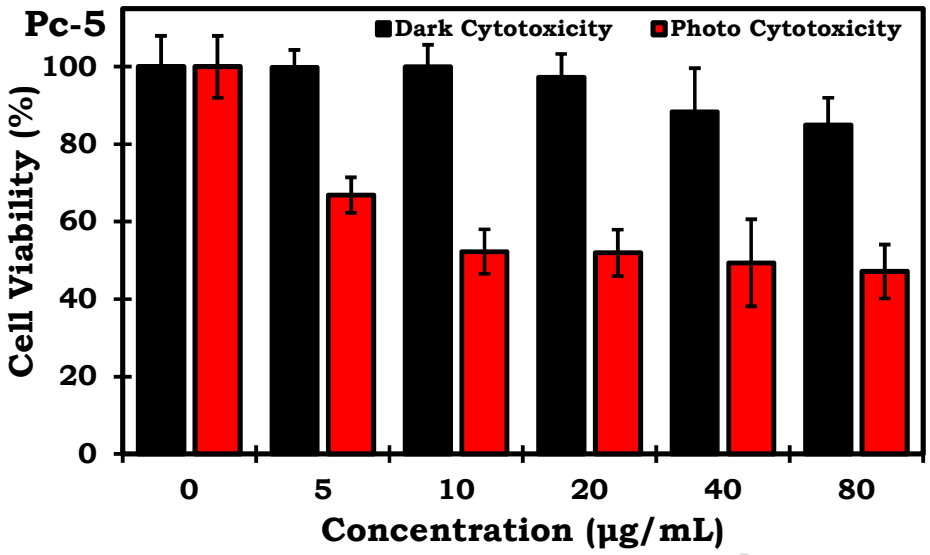

(B)

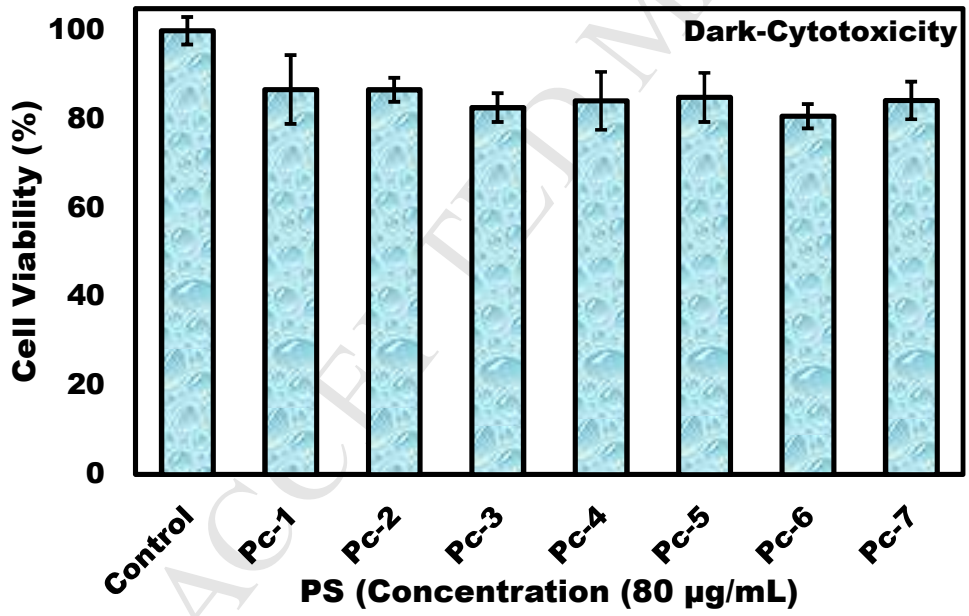

(C)

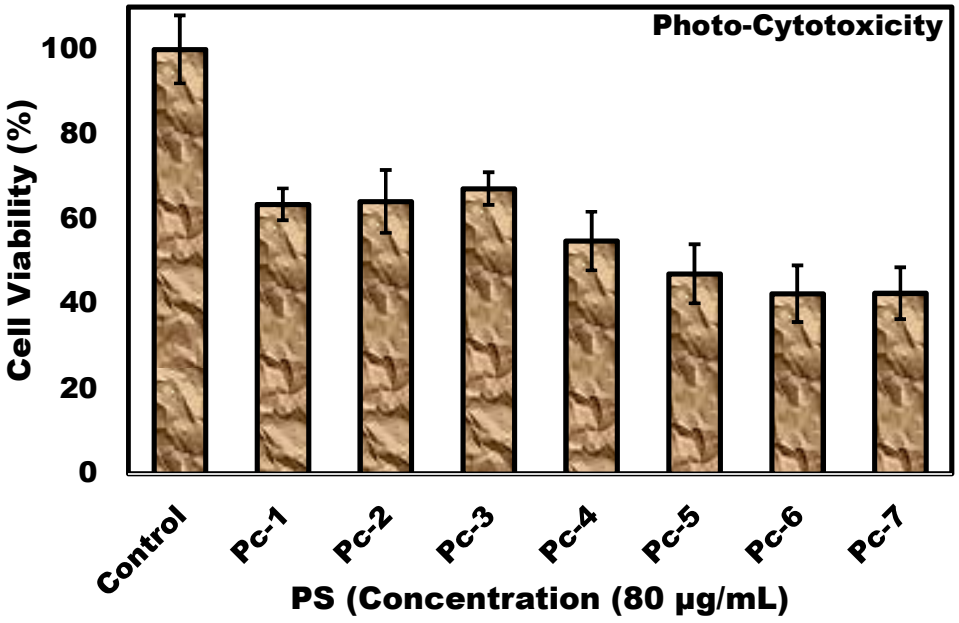

Figure 6

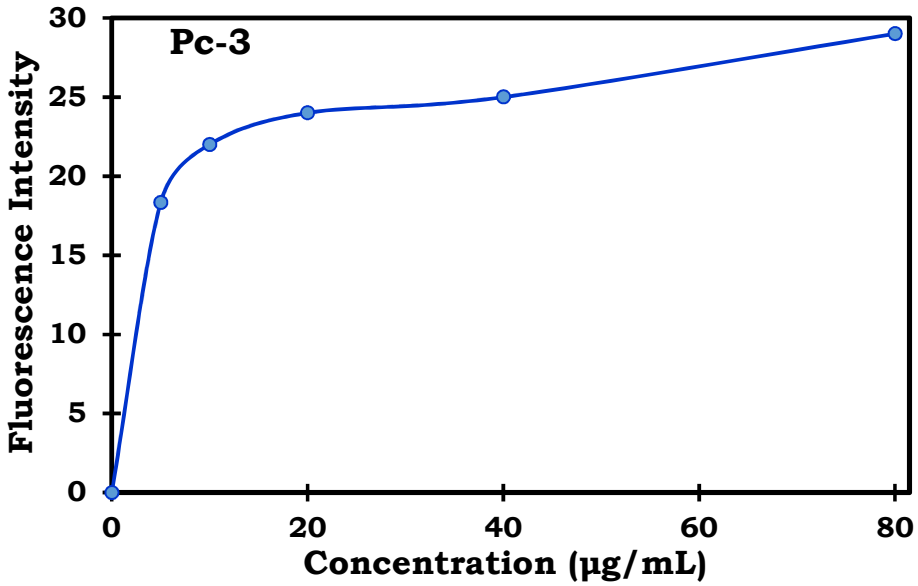

Figure 7

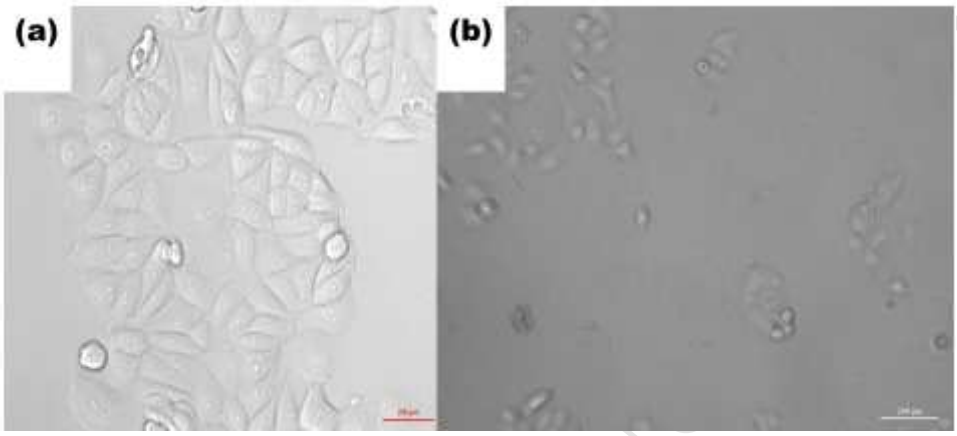

Figure 8:

Highlights:

- A novel thiol and oxy bridged phthalonitrile ligands were synthesized in their pure state.
- The ligands are used to synthesize corresponding substituted Zn and Al phthalocyanines.
- The complexes are used to study their photophysical and photochemical behaviour.
- The substituted ZnPc complexes afforded higher singlet oxygen quantum yields as compared to the AlPc analogue.
- All the complexes showed innocuous *invitro* dark cytotoxicity and moderate PDT effect against epithelial breast cancer cells.